TISSUE ENGINEERING: Part C
Volume 21, Number 5, 2015

DOI: 10.1089/ten.tec.2014.0377

Bone Morphogenetic Protein-2 Adsorption onto Poly-ε-caprolactone Better Preserves Bioactivity *In Vitro* and Produces More Bone *In Vivo* than Conjugation Under Clinically Relevant Loading Scenarios

Janki J. Patel, MS, Colleen L. Flanagan, MSE, and Scott J. Hollister, PhD

Background: One strategy to reconstruct large bone defects is to prefabricate a vascularized flap by implanting a biomaterial scaffold with associated biologics into the latissimus dorsi and then transplanting this construct to the defect site after a maturation period. This strategy, similar to all clinically and regulatory feasible biologic approaches to surgical reconstruction, requires the ability to quickly (< 1 h within an operating room) and efficiently bind biologics to scaffolds. It also requires the ability to localize biologic delivery. In this study, we investigated the efficacy of binding bone morphogenetic protein-2 (BMP2) to poly-ε-caprolactone (PCL) using adsorption and conjugation as a function of time.

Methods: BMP2 was adsorbed (Ads) or conjugated (Conj) to PCL scaffolds with the same three-dimensional printed architecture while altering exposure time (0.5, 1, 5, and 16 h), temperature (4°C, 23°C), and BMP2 concentration (1.4, 5, 20, and 65 μg/mL). The *in vitro* release was quantified, and C2C12 cell alkaline phosphatase (ALP) expression was used to confirm bioactivity. Scaffolds with either 65 or 20 μg/mL Ads or Conj BMP2 for 1 h at 23°C were implanted subcutaneously in mice to evaluate *in vivo* bone regeneration. Micro-computed tomography, compression testing, and histology were performed to characterize bone regeneration.

Results: After 1 h exposure to 65 μg/mL BMP2 at 23°C, Conj and Ads resulted in 12.83 ± 1.78 and 10.78 ± 1.49 μg BMP2 attached, respectively. Adsorption resulted in a positive ALP response and had a small burst release; whereas conjugation provided a sustained release with negligible ALP production, indicating that the conjugated BMP2 may not be bioavailable. Adsorbed 65 μg/mL BMP2 solution resulted in the greatest regenerated bone volume (15.0 ± 3.0 mm^3), elastic modulus (20.1 ± 3.0 MPa), and %bone ingrowth in the scaffold interior (17.2% ± 5.4%) when compared with conjugation.

Conclusion: Adsorption may be optimal for the clinical application of prefabricating bone flaps due to BMP2 binding in a short exposure time, retained BMP2 bioactivity, and bone growth adhering to scaffold geometry and into pores with healthy marrow development.

Introduction

THE GOLD STANDARD for reconstructing a bone defect is a vascularized autologous flap. However, this procedure results in donor site morbidity and poorly matched defect geometry, especially for craniofacial reconstruction. Alternatives to autografts include allografts and synthetic grafts. Allografts carry the risk of transferring diseases and eliciting an immune response. Synthetic grafts made from polymers or metal cages are alternatives being investigated to address the drawbacks of allografts and autografts. Particularly, polymers can be fabricated to match the patient's complex facial geometry and be integrated with biologics to induce bone growth when implanted into the defect site. Although these grafts could be readily available and produced, they do not integrate as well as autografts into the host bone.[1] Chronically infected and irradiated wound sites are challenging to reconstruct and are not conducive to general wound healing, let alone being able to support a bone graft. Furthermore, blood vessels generally cannot penetrate the graft sufficiently to provide nutrients to the bone growing at the graft's core, especially in large-volume defects. To increase viability and integration of grafts implanted directly into the defect site, researchers are investigating prefabrication of a synthetic flap that is assembled at a site remote from the defect.[2–5] As an alternative to creating the flap *in vitro* (in which patient cells are harvested, expanded, and seeded on the construct to mature in an external bioreactor),

Department of Biomedical Engineering, University of Michigan, Ann Arbor, Michigan.

we are looking to tissue engineer a bone flap *in vivo* by using the patient's body as a bioreactor to achieve bone penetration into a biomaterial scaffold with associated biologics. There are a few reports of this procedure in animal models[4,6–10] and even less in humans.[2,3,11] Previous studies have used BioOss/Hydroxyapatite blocks or titanium trays filled with BioOss blocks soaked in growth factors (GF).[7,8] A human mandibular case using a titanium mesh filled with hydroxyapatite blocks soaked in bone morphogenetic protein-7 (BMP7) fractured and failed.[2]

Our goal is to advance this prefabricated flap procedure by integrating patient-specific computational design, three-dimensional (3D) biomaterial printing, and postfabrication biologic functionalization.[12] Poly-ε-caprolactone (PCL) is a biocompatible and bioresorbable polymer that can be utilized with image-based computation-aided design and selective laser sintering (SLS) manufacturing techniques.[13] SLS can repeatedly and reproducibly produce PCL scaffolds with complex geometries, controlled pore size, and stiffness that degrade over 3 years. Its degradation profile and mechanical properties support its use for bone tissue engineering in complex reconstruction sites where bone may take over a year to form. In these sites, a PCL scaffold's slower degradation time is an advantage to provide form and load bearing over a longer time period. Furthermore, PCL degradation generates less acidic byproducts and leads to less inflammation than more rapidly degrading polylactic acid-based co-polymers.[14] PCL has been approved for cranioplasty bone-filling applications by the FDA.[15,16] Thus, the polymer has been widely tested, utilized, and achieved regulatory approval as a bone repair scaffold. Furthermore, it may readily be formed into complex geometries by 3D printing techniques such as SLS and Fused Deposition Modeling.[17–20]

PCL can be modified to integrate the osteoinductive agent recombinant human bone morphogenetic protein-2 (BMP2).[21,22] However, further studies are needed to refine a method of GF functionalization onto PCL scaffolds to produce bone when placed in the muscle bed (i.e., prefabricated flap applications) in a clinically realistic time frame within the operating room (OR). Although a plethora of methods have been developed for conjugating and delivering BMP2 from scaffold materials, any conjugation technique requiring more than 1 h and performed outside the OR faces unknown sterilization effects on GF bioactivity and creates a significant uphill battle to be of any clinical relevance. It is likely that any clinically relevant BMP2 delivery method for the near future should be performed in the OR environment at room temperature with loading times of 1 h or less. Current conjugation methods that more efficiently load BMP2 onto scaffolds than adsorption methods[23,24] do not fulfill these requirements. In addition, studies that have assessed conjugation methods utilized either porogen leaching[22,23] or other methods, resulting in large variations in pore architecture that may significantly affect release kinetics, not allowing a rigorous comparison of adsorption and conjugation methods.[25–27] Simpler adsorption methods have not been directly compared with conjugation methods.[27–29] Still, there is a lack of information on how conjugation methods could be compared directly with adsorption methods under OR relevant conditions on scaffolds with the exact same, rigorously controlled architecture in terms of not only *in vitro* loading efficiency and bioactivity but also the direct translation into *in vivo* bone formation in terms of volume, localization, and mechanical properties. The goal of this study was to investigate these questions both *in vitro* and in an *in vivo* ectopic model as a precursor to large animal ectopic models for prefabricated flap construction.

Materials and Methods

PCL fabrication

PCL discs (15 mm diameter, 2 mm height, and 176 mm^2 surface area) and 70% porous scaffolds (6.35 mm diameter $\times$ 4 mm height, 170 mm^2 surface area) with 2.15 mm spherical pores (Fig. 1) in a 2 mm unit cell were fabricated using a Formiga P100 SLS machine (EOS, Inc.). The powder consisted of PCL (43–50 kDa; Polysciences) and 4 wt% hydroxyapatite (Plasma Biotal Limited). Manufacturing conditions, including bed temperature, laser power, particle size, and PCL milling, followed protocols that had been previously developed and published for implantable PCL scaffolds.[13,17,30,31] After manufacturing, the discs and scaffolds were air blasted and then sonicated in 70% ethanol (EtOH) for 30 min to remove nonsintered powder, washed in distilled water (diH_2O), and air dried at room temperature.

BMP2 binding

For conjugation groups (Conj), PCL samples were exposed to 10% w/v 1,6-hexanediamine in isopropanol for 1 h at 37°C to add amine groups via aminolysis and then they were washed in diH_2O. After air drying overnight, 1 M Ninhydrin reagent (Sigma), prepared with 100% EtOH, was used to confirm successful aminolysis in a representative specimen by development of a purple stain. Note that this preparation can be done presterilization and does not affect the capability to perform conjugation under OR relevant conditions. The samples were prewashed with activation buffer (BuPH Phosphate-Buffered Saline Pack in diH_2O, pH 7.2 Pierce Biotechnology). The heterobifunctional crosslinker sulfosuccinimidyl 4-(N-maleimidomethyl) cyclohexane-1-carboxylate (sulfo-SMCC; Pierce Biotechnology) was used to immobilize recombinant human BMP2 (*Escherichia coli* derived; Creative Biomart) on the aminated surface. Samples were immersed in sulfo-SMCC (4 mg/mL in activation buffer) for 1 h at 23°C, followed by activation and conjugation buffer washes. Conjugation buffer (pH 7.0) contained activation buffer and 0.1 M EDTA. Adsorption

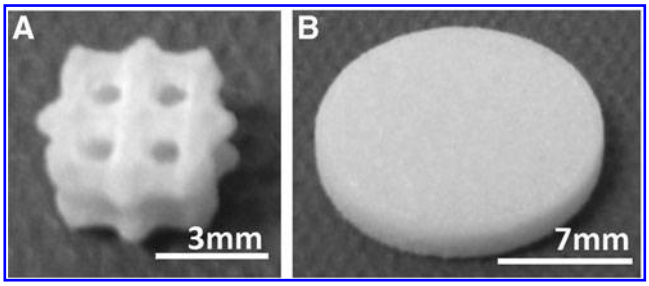

FIG. 1. **(A)** PCL scaffold **(B)** PCL disc. PCL, poly-ε-caprolactone.

groups (Ads) followed the same procedure as Conj but without the aminolysis and sulfo-SMCC reactions. *E. coli*-derived BMP2 is nonglycosylated and has been shown to produce more bone *in vivo* at a lower dose when compared with a glycosylated BMP2.[32] BMP2 was dissolved in 20 mM acetic acid (1 mg/mL) and then further diluted in conjugation buffer to the desired concentration. Ads/Conj PCL discs ($n=3$/group) were immersed in 1 mL of 1.43 μg/mL BMP2 solution for 0.5, 1, 5, or 16 h on a shaker at 4°C or 23°C. A simple disc geometry was used to understand initial binding trends before conducting concentration binding studies with a refined protocol on a more complex geometry. Ads/Conj PCL scaffolds ($n=3$/group) were immersed in 1 mL of 1.4, 5, 20, or 65 μg/mL BMP2 for the refined conditions of 1 h exposure at 23°C. Note that an enzyme-linked immunoabsorbant assay (ELISA) was used to determine the detected BMP2 concentration (averaging 1.14, 3, 6.5, and 30 μg/mL) with which to normalize binding values. Once BMP2 exposure was complete, samples were washed with diH_2O and dried in a vacuum at 23°C overnight. BMP2 solution supernatants and diH_2O washes were collected in LoBind microcentrifuge tubes (Eppendorf) to analyze for BMP2 content. Bovine serum albumin (BSA) 1% was added to the collected solution to result in 0.1% BSA, and the samples were stored at −80°C. BMP2 content was quantified using an indirect ELISA kit (PeproTech) read at 405 and 650 nm on a microplate reader (Multiskan Spectrum; Thermo Scientific). Results are reported as BMP2 bound (μg), BMP2 bound per mm^2 PCL surface area (μg/mm^2), or binding efficiency (%) and were calculated as shown next:

$$\begin{aligned} BMP2\ Bound\ (\mu g) = {} & BMP2\ in\ original\ solution \\ & detected\ by\ ELISA \\ & -(BMP2\ in\ supernatant + washes) \end{aligned}$$

$$Binding\ Efficiency\ (\%) = \left(\frac{original\ Amt - Amt\ remaining\ in\ sol'n}{original\ Amt}\right) * 100$$

Release kinetics

Ads and Conj BMP2 release profiles were determined for PCL scaffolds exposed to 20 μg/mL BMP2 for 1 h at 23°C ($n=3$). After BMP2 exposure, PCL samples were immersed in Dulbecco's phosphate-buffered saline (DPBS) and incubated in a sterile environment at 37°C, 5% CO_2, and 95% humidity. The supernatant was collected and replaced with fresh DPBS at 1, 3, 5, 7, 14, and 21 days after initial exposure. Supernatant with added 0.1% BSA was stored at −80°C until BMP2 quantification by ELISA.

BMP2 quantification

An *E. coli*-derived BMP2 ELISA quantification kit (Peprotech) was used to indirectly quantify the amount of BMP2 bound to PCL and was conducted according to the manufacturer's instructions. High-binding 96-well plates (Costar) were coated with capture antibody overnight. Wells were blocked with 1% BSA in DPBS for 1 h; thawed samples were added in triplicate wells for 2 h, detection antibody for 2 h, and Avidin-conjugated horseradish peroxidase for 0.5 h, followed by the addition of ABTS liquid substrate solution (2,2′-azino-bis(3-ethylbenzthiazoline)-sulfonic acid; Sigma) for colorimetric reading after 20 min. In between each step, wells were washed four times with wash buffer (DPBS containing 0.05% Tween 20; Sigma). Absorbance was read at 405 and 650 nm.

Cell culture

C2C12 myoblastic cells are known to differentiate down an osteogenic lineage when exposed to active BMP2 and are extensively used in other studies as an initial screening of BMP2 bioactivity.[33–36] C2C12 cells (ATCC) were grown in high-glucose Dulbecco's modified Eagle's medium (DMEM) containing 10% fetal bovine serum and 1% penicillin/streptomycin and incubated at 37°C, 5% CO_2, and 95% humidity (all reagents from Gibco). The Ads and Conj BMP2 discs were sterilized in 0.22 μm-filtered 70% EtOH for 30 min, washed with Hanks balanced salt solution (HBSS), and maintained in DMEM under sterile conditions until cell seeding in a 24-well plate. Discs fit tightly into the well space. The DMEM was then replaced with culture medium, and cells were added.

Alkaline phosphatase assay

C2C12 cells were seeded (1×10^4 cells/disc or 57 cells/mm^2) on discs with conjugated or adsorbed 0.7 mL of 1.4 μg/mL BMP2 for 1 h at 23°C. Simple disc geometry was used for cell studies, because the aim of the study was to determine whether the bound BMP2 maintained bioactivity and the extent of bioactivity was not compared. Positive controls were 1 μg BMP2 in culture medium (sol BMP2) and 0.7 mL of 1.4 μg/mL BMP2 adsorbed for 16 h at 4°C due to earlier successful results in this laboratory for *in vivo* formation at that binding condition ($n=4$). The negative controls were cells on PCL discs with no BMP2. After 4 days of static culture, cells were lysed with 700 μL of Cel-Lytic (Sigma) solution and alkaline phosphatase (ALP) production was quantified. The assay was conducted using alkaline buffer solution, p-nitrophenol standard solution, and ALP substrate tablets (Sigma). Each sample ($n=3$/group) was read in triplicate wells at 405 nm, and results were normalized to total intracellular protein content (BCA ThermoScientific) read at 562 nm.

MTS assay

An MTS assay was utilized to ensure cells attached and grew on the PCL to interact with the bound BMP2. Proliferation between groups was not compared. C2C12 cells were seeded (2.5×10^4 cells/disc) on discs with Conj or Ads 1.43 μg/mL BMP2 for 1 h at 23°C and Ads at 4°C ($n=4$). The positive controls were cells seeded on PCL discs exposed to 1 μg BMP2 in culture medium (sol BMP2). The negative controls were cells on PCL discs with no BMP2. Two hundred sixty microliters of MTS solution (CellTiter96 Aqueous One Solution; Promega) were added to each disc after 72 h of static culture. After incubation for 2 h at 37°C, triplicates were read at 490 nm.

In vivo *bioactivity: subcutaneous implantation*

Based on our *in vitro* studies, we chose the most clinically relevant conditions of 1 h protein exposure at 23°C and exposed scaffolds to 20 or 65 μg/mL adsorbed or conjugated BMP2. After treatment, scaffolds were implanted subcutaneously in 5–7 week-old NIHS bg-nu-xid mice (Harlan Laboratories). Negative controls for the adsorption group were PCL scaffolds soaked in conjugation buffer for 1 h. Negative controls for the conjugation group were PCL scaffolds treated through the sulfo-SMCC reaction step without BMP2 exposure. Groups were sterilized with 70% EtOH and washed with HBSS before implantation. Four scaffolds were implanted in each mouse. An incision was made in the back, and four pockets were created angling toward each limb. Scaffolds were assigned a quadrant to be implanted in such that at least one sample from each group was implanted in all quadrants. Mice were then euthanized at 8 weeks postsurgery to explant the specimen. Explanted specimens were placed in Z-Fix (Anatech) overnight, washed with diH_2O for 5 h, and stored in 70% EtOH until testing. Table 1 gives total sample numbers as well as the number of samples used for each specific assay (microCT scan, mechanical test, and histology). This study was conducted in compliance with the regulations set forth by the University Committee on Use and Care of Animals at the University of Michigan.

Micro-computed tomography

Fixed scaffolds were scanned in water with a high-resolution micro-computed tomography (microCT) scanner (Scanco Medical) at 16 μm resolution, and scans were calibrated to Hounsfield units (HU). Bone volume (BV), tissue mineral density (TMD), and tissue mineral content (TMC) data were determined. Bone was defined at a threshold of HU = 1050 using Microview software (Parallax Innovations). TMD is an assessment of bone quality within the scaffold; the measure indicates the average density of the bone tissue (as defined by the threshold value of 1050 HU) within a given 3D region of interest (ROI) and is reported as the mass of hydroxyapatite per volume (mgHA/mm^3). TMC quantifies the amount of mineral present in the bone (as defined by the threshold value of 1050 HU) in a given ROI and is reported as the mass of hydroxyapatite (mgHA). To obtain TMD and TMC values, Dicoms from Scanco were imported into Microview and grayscale values for each voxel were exported to excel and be converted to HU values. The scaffold region was represented as a cylindrical ROI (6 × 3.615 mm). Bone formed outside the scaffold ROI boundary was quantified and defined as ''external'' bone growth, and bone inside the scaffold ROI was defined as ''internal'' BV. External, internal, and total BV, TMD, and TMC were calculated for each specimen.

To determine bone penetration into the scaffold radially, four concentric, cylindrical rings were defined as ROIs and were individually analyzed with regard to BV and TMC. The diameters of the four concentric rings are as follows: Ring 1: 6.00–4.84 mm, Ring 2: 4.84–3.67 mm, Ring 3: 3.67–2.5 mm, and Ring 4: 2.50–0.00 mm. BV, and bone ingrowth of each ring were calculated using Microview Software. Bone ingrowth (%) was calculated as BV divided by the available pore volume for each ring. Available pore volume was calculated from the porosity of each ring based on the .STL design file for the scaffold.

Table 1. Sample Numbers for *In Vivo* Analysis Number of Samples Used in Explanted Specimen Analysis Methods

Group	*microCT scan*	*Mechanical test*	*Histology*	*Total samples*
20 μg/mL Conj	$n=8$	$n=5$	$n=3$	$n=8$
65 μg/mL Conj	$n=9$	$n=6$	$n=3$	$n=9$
20 μg/mL Ads	$n=8$	$n=5$	$n=3$	$n=8$
65 μg/mL Ads	$n=9$	$n=6$	$n=3$	$n=9$
PCL-no BMP2	$n=5$	$n=3$	$n=2$	$n=5$
Sulfo-SMCC	$n=9$	$n=6$	$n=3$	$n=9$

Ads, adsorption; BMP2, bone morphogenetic protein-2; Conj, conjunction; microCT, micro-computed tomography; PCL, poly-ε-caprolactone.

Compression mechanical testing

Specimens were mechanically tested using an MTS Alliance RT30 electromechanical test frame (MTS Systems Corp.) with a 500 N load cell. Samples were compressed between two steel platens at a rate of 1.0 mm/min with a 0.5 lbf preload. Data were collected and analyzed using TestWorks4 software (MTS Systems, Corp.). Data were collected to a 25% strain, and the compressive elastic modulus was defined as the slope of linear region of the stress-strain curve before the 15% strain. Data were normalized to scaffold area.

Histology

Fixed samples from each group were decalcified with RDO (Sigma) and sent to the Histology Core at the University of Michigan Dental School to be embedded in paraffin, sectioned, and stained with hematoxylin and eosin (H&E). H&E was used to visualize cells, tissue matrix, blood vessels, and general tissue morphology. A light microscope was used to image sections at 10× magnification.

Statistical analysis

Data are expressed as mean ± standard deviation of the mean. An analysis of variance was used to determine statistical significance between groups. A *p-value < 0.05 ($\alpha < 0.05$) was considered statistically significant on a 95% confidence interval.

Results

Binding environment studies

At 4°C, conjugation had significantly more BMP2 attached than adsorption at all exposure times. At 23°C, conjugation still had significantly higher binding at 0.5 and 1 h exposures. Adsorption at 23°C resulted in significantly more BMP2 bound than at 4°C except at the 16 h exposure. After 1 h exposure at 23°C, conjugated and adsorbed discs resulted in 0.0049 ± 0.001 μg/mm^2 ($99.5\% \pm 0.1\%$) and 0.0036 ± 0.0001 μg/mm^2 ($73.3\% \pm 1.3\%$) BMP2 attached, respectively (Fig. 2). Based on these results, we examined Conj/Ads groups that were exposed to BMP2 for 1 h at 23°C in further studies.

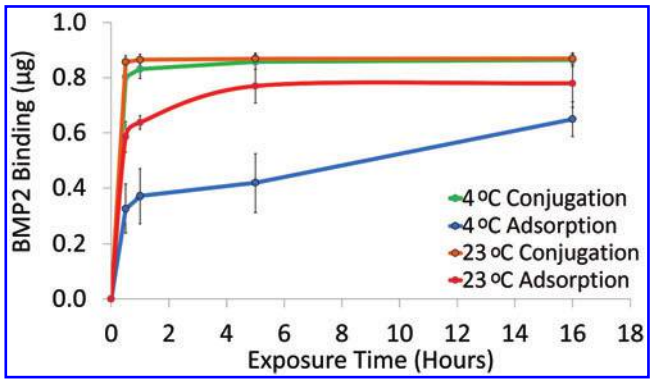

FIG. 2. BMP2 binding to PCL discs via adsorption or conjugation. PCL discs were exposed to 1.4 µg/mL BMP2 solution for 0.5, 1, 5, or 16 h at 23°C or 4°C. BMP2 was quantified with an ELISA ($n=3$). BMP2, bone morphogenetic protein-2; ELISA, enzyme-linked immunoabsorbant assay. Color images available online at www.liebertpub.com/tec

BMP2 in vitro bioactivity

To determine whether the bound BMP2 was nontoxic and bioactive, we seeded C2C12 myoblastic cells on BMP2 Ads or Conj PCL discs. We found that cells on all PCL discs proliferated significantly more than the negative control (Fig. 3A). Cells on adsorbed groups produced significantly higher ALP than the conjugated group. ALP production of cells on PCL without BMP2 was the same as conjugation and significantly less than adsorption. There was no difference between discs that had BMP2 adsorbed at 4°C or those at 23°C ($p=0.10$). Finally, the positive control of soluble BMP2 in cell culture medium showed significantly higher ALP (1.16 nM ALP/mg protein/min) compared when with all other groups (Fig. 3B).

Concentration binding studies

For a transition to *in vivo* bioactivity studies, 70% porous scaffolds (176 mm^2) were exposed to increasing BMP2 concentrations for 1 h at 23°C (adsorbed and conjugated). The BMP2 bound to scaffolds was compared with the amount adsorbed onto a disc (170 mm^2). There was no significant difference in binding between adsorbed/conjugated scaffolds and discs at 5, 20, and 65 µg/mL. Significantly more BMP2 bound to the surface as BMP2 concentration increased (Fig. 4A). When exposed to 20 µg/mL BMP2, 3.03 ± 0.18 µg (0.018 ± 0.001 µg/mm^2) BMP2 attached with conjugation and 2.49 ± 0.35 µg (0.015 ± 0.002 µg/mm^2) attached with adsorption. When exposed to 65 µg/mL, conjugation and adsorption bound 12.83 ± 1.78 µg (0.076 ± 0.01 µg/mm^2) and 10.78 ± 1.49 µg (0.063 ± 0.01 µg/mm^2) BMP2, respectively. Figure 4B shows the percentage of BMP2 in the original solution that bound to the scaffold surface (% binding efficiency). Conjugation bound significantly more BMP2 than adsorption when exposed to 1.4 µg/mL. There was no difference in amount bound between the two methods as BMP2 concentrations increased to 5, 20, and 65 µg/mL.

In vitro *release kinetics*

A carrier device's release kinetics plays a crucial role in the quality of engineered bone. PCL scaffolds exposed to 20 µg/mL BMP2 solution for 1 h at 23°C showed that after 22 days, 0.0026 ± 0.0006 and 0.0167 ± 0.005 µg of conjugated and adsorbed BMP2 was released, respectively (Fig. 5A). A burst release commonly observed with adsorption occurred in the first 1–3 days, during which about 0.0068 µg BMP2 was released (Fig. 5B).

In vivo *bone formation*

After 8 weeks of subcutaneous implantation, we found that adsorbed PCL scaffolds exposed to 20 and 65 µg/mL BMP2 solution produced the greatest total BV of 9.2 ± 2.28 and 15.02 ± 2.98 mm^3, respectively. Conjugation produced 0.43 ± 0.41 and 5.9 ± 2.0 mm^3 total bone when exposed to 20 or 65 µg/mL, respectively. Negative control blank PCL produced significantly less bone (0.14 ± 0.03 mm^3) than all other groups (Fig. 6A). Using Microview to visualize microCT scans of explanted specimen, we found that conjugation produced a shell of bone that followed scaffold geometry. Adsorption resulted in bone following scaffold geometry as well as filling into the pores (Fig. 6B). The bone formed outside of the scaffold ROI for 65 µg/mL adsorption (1.42 ± 0.52 mm^3) and 65 µg/mL conjugation (0.14 ± 0.08 mm^3) was not excessive (Fig. 6A, B).

Sixty-five µg/mL adsorbed also had significantly higher TMC (8.44 ± 1.7 mg HA) than other groups. Finally, 65 µg/mL conjugated, 20 µg/mL adsorbed, and 65 µg/mL adsorbed produced bone that is within the normal density range of

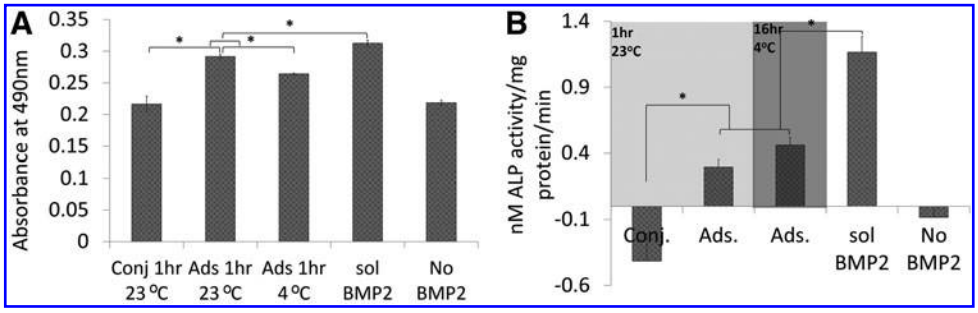

FIG. 3. BMP2/PCL cytotoxicity and bioactivity. **(A)** MTS assay results for relative C2C12 proliferation on BMP2/PCL discs. Cells were able to grow on PCL surface modified with BMP2 ($n=4$). **(B)** ALP production of C2C12 cells seeded on BMP2/PCL discs. Data are normalized to total intracellular protein content and based on linear curve fit. *$p<0.05$ was significant. ALP, alkaline phosphatase.

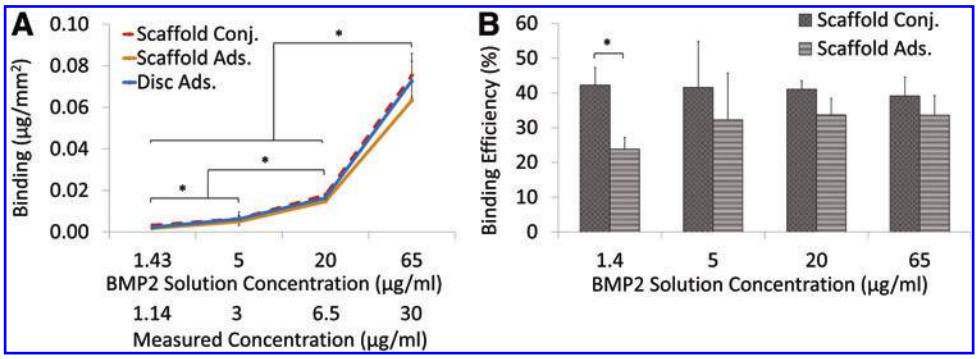

FIG. 4. BMP2 binding to PCL discs and scaffolds. **(A)** PCL scaffolds were exposed to 1.43, 5, 20, or 65 μg/mL BMP2 solution for 1 h at 23°C. The data were normalized to the ELISA detected concentration, which averaged at 1.14, 3, 6.5, and 30 μg/mL. *$p < 0.05$. **(B)** Bound BMP2 is expressed as a percentage of BMP2 in original solution ($n = 3$). Color images available online at www.liebertpub.com/tec

mandibular bone (551 ± 25, 587 ± 25, and 560 ± 37 mg HA/cm^3, respectively).[13,37]

Ring analysis showed a similar relationship in that adsorption resulted in higher %bone ingrowth in all rings when compared with conjugation. Percent bone ingrowth was the same throughout the scaffold for 65 μg/mL adsorption. At the center of the scaffold, 65 μg/mL adsorption and conjugation had 17.2% ± 5.4% and 7.5% ± 3.07% ingrowth, respectively (Fig. 7).

Mechanical testing

As seen in Figure 8, nearly all groups had significantly higher moduli when compared with the blank PCL (12.7 ± 1.1 MPa) or sulfo-SMCC negative controls, with the exception of 20 μg/mL conjugated ($p = 0.12$). The 65 μg/mL adsorbed group had the highest elastic modulus of 20.1 ± 3.0 MPa, which was significantly higher than the 65 μg/mL conjugated group (15.1 ± 1.3 MPa). However, at a lower concentration level, there was no difference between 20 μg/mL conjugated and 20 μg/mL adsorbed moduli.

Histology

Scaffold pores of sulfo-SMCC, blank PCL, and 20 μg/mL conjugated BMP2 were infiltrated primarily with fibrous and fatty tissue (Fig. 9). Negligible bone formation was observed in these groups. However, both of the adsorbed groups (20 and 65 μg/mL) showed blood, bone, and fatty marrow growth into the scaffold pore space. There were multiple osteocytes embedded in the osteoid as well as osteoblasts lining the matrix. The 65 μg/mL conjugated group showed bone growth, fibrous tissue, and a little fatty marrow as well; however, the resulting bone was primarily localized to the pore surface and did not grow into the pores as well as the adsorbed group.

Discussion

Prefabricating a bone flap *in vivo* has been completed in Europe and Asia, but to the best of our knowledge, it has not yet been completed in the United States. For the foreseeable future, this will likely be the method that can best generate large vascularized bone constructs for reconstruction. Medtronic's product Infuse™ has been FDA approved for delivery of BMP2 from a collagen type 1 sponge in treatment of spinal fusion, open tibial fractures, sinus augmentation, and dental procedures.[38] Due to BMP2's short half-life, a 1.5 mg/mL BMP2 dose was needed (greatly exceeding native concentrations of 18.8–22 pg/mL), which resulted in a large burst release during the first 2–3 days, causing adverse reactions in some patients.[39] To control the release and prevent excessive bone growth, Park *et al.* chemically conjugated BMP2 to amine-containing chitosan with a

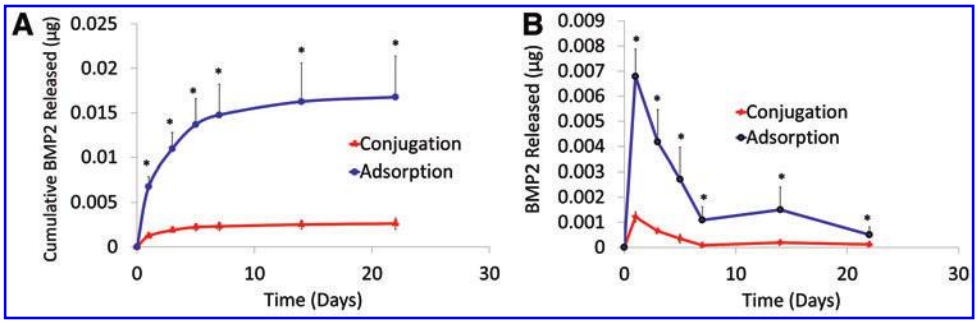

FIG. 5. Conjugated and adsorbed BMP2 released from PCL. **(A)** Cumulative release of BMP2 from PCL scaffolds into DPBS when exposed to 20 μg/mL BMP2 for 1 h at 23°C. Release environment conditions were sterile, 37°C, 5% CO_2, and 95% humidity. *$p < 0.05$. **(B)** BMP2 (μg) released per day. The supernatant was analyzed for BMP2 content with an ELISA ($n = 3$). DPBS, Dulbecco's phosphate-buffered saline. Color images available online at www.liebertpub.com/tec

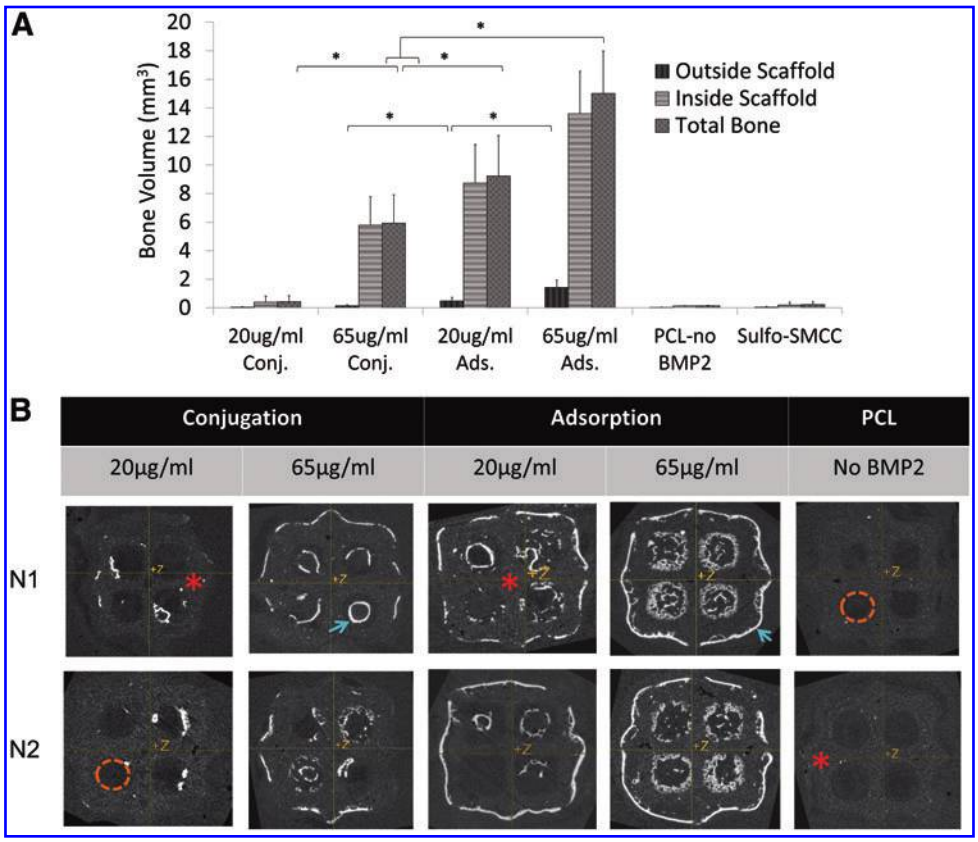

FIG. 6. Regenerated Bone Analysis. **(A)** Microview Software analysis for bone volume formed in explanted specimen using microCT scans (threshold = 1050 HU). ''Inside scaffold'' was defined as bone volume inside a cylindrical ROI (6 mm D, 3.615 mm H), and ''outside scaffold'' was the bone volume formed outside the ROI. **(B)** Microview Software Visual Analysis of microCT Scans. Two representative samples from each group are shown. *Bright white areas* indicate bone formation (*blue arrow*), and *gray areas* are scaffold (*red**). *Dark areas* (*orange dashed lines*) indicate pores. Conjugation produced bone that closely followed PCL surface geometry. Adsorption produced bone growth into the pores in addition to following surface geometry. *$p < 0.05$. HU, Hounsfield units; microCT, micro-computed tomography; ROI, region of interest. Color images available online at www.liebertpub.com/tec

sulfo-SMCC cross-linker. Conjugation enhanced *in vitro* osteoinductive properties as determined by preosteoblast differentiation; however, chitosan would not be an ideal carrier for creating a bone flap, because it lacks mechanical integrity.[25] BMP2 adsorption and conjugation via heparin and sulfo-SMCC onto uncoated polymer surfaces (PLGA and PCL) has been superficially compared, but a study was needed to refine a simple BMP2-binding method onto 3D SLS manufactured PCL scaffolds in a clinically applicable environment.[22,23]

In this study, we aimed at refining a protocol for binding BMP2 to PCL, considering the constraints of intra OR use and for testing bone regeneration using the sulfo-SMCC and simple adsorption binding protocols *in vivo*. Studies have used various methods to deliver BMP2 from biomaterials, including sulfo-SMCC, heparin, trauts, adsorption, and incorporation into a coating or microparticles.[24,26,29,36,40–44] Temperatures and exposure times at which protein binding studies have been tested range from 4°C to 37°C and from 1 h to 24 h.[25,36,45,46] However, temperatures outside room temperature and long exposure times make it very difficult to use such BMP2 conjugation methods clinically. In this study, we found that chemical conjugation with sulfo-SMCC bound more BMP2 during a shorter exposure time and at ambient temperature in comparison to adsorption; however, the conjugated BMP2 did not maintain bioactivity once bound to the surface as determined by an absence of ALP production *in vitro*. This inactivity could be due to the sulfo-SMCC binding reaction binding BMP2 in a conformation that does not ideally present its cell-binding moiety.

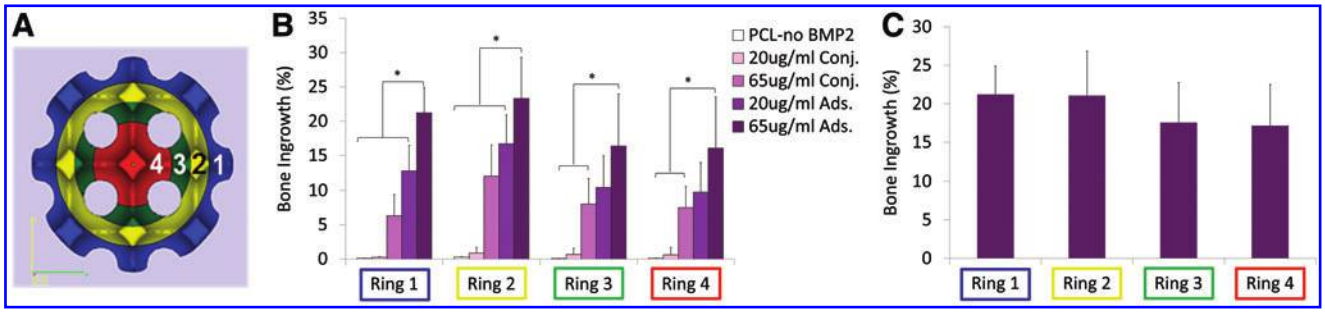

FIG. 7. Ring Analysis for Bone Growth into Scaffold. **(A)** Outer ROI diameters were 6.0, 4.84, 3.67, and 2.50 mm for Rings 1, 2, 3, and 4, respectively. **(B)** Percentage bone ingrowth (bone volume divided by available pore space) showed that 65 µg/mL adsorbed group had significantly more ingrowth than either of the conjugated groups. **(C)** Sixty-five µg/mL adsorbed group resulted in the same bone penetration throughout the scaffold. *$p < 0.05$. Color images available online at www.liebertpub.com/tec

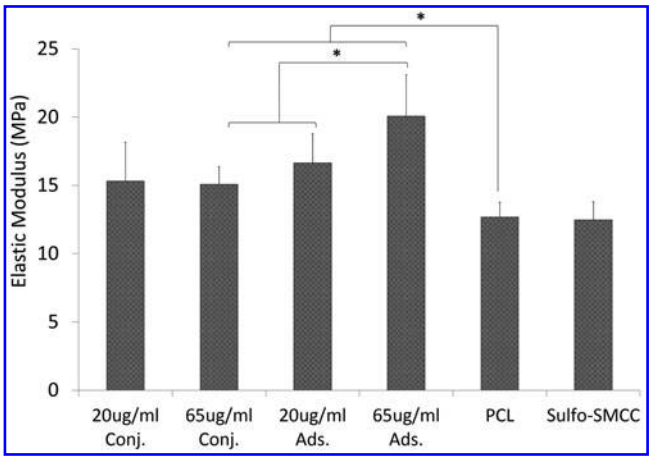

FIG. 8. Compressive mechanical testing. Specimen elastic modulus measured in compression was defined as the slope of linear region before 15% strain level and normalized to specimen surface area. $*p < 0.05$.

Even though adsorbed BMP2 may not have bound as efficiently as conjugated BMP2 at 23°C, it was shown to be bioactive *in vitro* and produced more bone that infiltrated the scaffold and pores *in vivo.* We also showed that adsorbed BMP2 bound more efficiently at 23°C than at 4°C, which is a clear advantage for the intra OR setting. This increased binding may have been due to increased protein kinetics providing the protein with more opportunities to bind to the material surface.

GF delivery vehicle release kinetics are crucial to the resulting bone formed. Conjugation resulted in sustained GF release, whereas adsorption had a slightly higher burst release after 1–3 days, followed by a sustained release over time. This burst release with adsorption is commonly seen in other studies[26,27,36]; however, in this case when BMP2 is delivered from laser sintered PCL, the amount released, in a burst and during subsequent slower release, at the secondary site is extremely small (<1%), which is much smaller than the other studies.[26,36,46] The released amount is still therapeutically relevant, because the regenerated bone increased the scaffold's load-bearing abilities. Since the *in vitro* release was at 37°C, the remaining BMP2 could have degraded and the ELISA may not have detected the BMP2 fragments. Although an ELISA is a widely used method to detect low BMP2 concentrations, an alternate detection method that could be utilized to confirm the release kinetics would be to use ^{125}I-labeled BMP2.[25] Overall, adsorption provided greater BMP2 release over time. A limitation to this study was that the *in vitro* release profile may not entirely accurately predict the *in vivo* release profile due to physiological factors such as enzymes cleaving BMP2 off the surface.

For a transition to *in vivo* studies and to confirm BMP2 bioactivity, we increased the amount of BMP2 exposed to PCL and used a more complex geometry. We determined the same amount of BMP2 adsorbed onto discs as onto scaffolds and that samples bound increasingly more μg BMP2/mm^2 when they were exposed to increasing BMP2 concentrations. The higher concentrations may have caused a stronger concentration gradient which drove adsorption at a rate similar to that of conjugation. The *in vivo* study showed that adsorption on PCL may be more clinically applicable, because not only did bone formation follow scaffold surface geometry similar to conjugation but it also grew into the interior available pore space. This increased bone ingrowth is likely the reason that adsorption had a higher elastic modulus than conjugation groups. This superior mechanical integrity will be crucial once the bone flap is transferred to the defect site. Adsorption also provided the most overall bone growth as well as bone formed at the center of the scaffold. When applied to a bone flap model, it is important to produce as much bone as possible before transferring it to assist the flap to integrate into the defect site as well as to facilitate further bone remodeling and growth. The ectopic model for bone regeneration was, due to our interest in prefabricated flaps, the process by which we wanted to test BMP2 delivery.

This scaffold was acellular when implanted; therefore, we speculate that circulating cells such as mesenchymal stem cells and fibroblasts which migrated through the vasculature in the wound bed could have interacted with the released BMP2 and were involved in endochondral bone formation. Due to a lack of bioactivity exhibited *in vitro,* but the presence of bone formed *in vivo*, we believe that conjugated BMP2 may be released via proteolytic activity and adsorption may release the protein through weak molecular interactions.

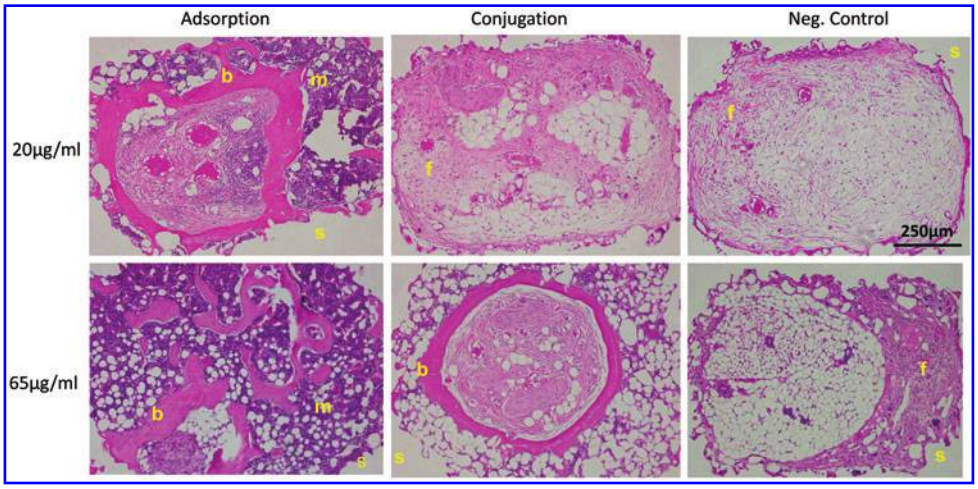

FIG. 9. Hematoxylin and eosin images of PCL/BMP2 scaffold pores. Bright-field images of scaffold pores taken at 10× magnification. b, bone; f, fibrous tissue; m, marrow; s, scaffold. Negative controls consisted mainly of fibrous tissue. Color images available online at www.liebertpub.com/tec

Overall, adsorption onto PCL makes BMP2 available faster to cells than conjugation via sulfo-SMCC. In the future, we would like to determine a dual GF delivery system to increase the bone growth rate into the scaffold so that the flap can be transplanted at an earlier time point for oncology patients waiting for adjunct therapy.

Conclusions

To address the drawbacks associated with autographs, allografts, and synthetic grafts, we propose the idea of prefabricating a flap that is autologous in nature. The ability to create complex PCL geometries for craniofacial reconstruction is an advance in prefabricating flaps, as only crude geometries were utilized in other cases. Based on these studies, adsorbing BMP2 onto PCL may be more optimal for clinical use in comparison to conjugation via sulfo-SMCC due to BMP2 binding in a short exposure time at ambient temperature, retained BMP2 bioactivity, bone growth following scaffold geometry and into pores, and healthy marrow development. Further studies are currently being conducted to determine whether these *in vivo* results can be replicated in a large porcine model and, furthermore, transplant the PCL implant to a mandibular angle defect. We will compare the prefabricated flap results to a PCL implant placed directly into the defect site.

Acknowledgments

This research was funded by the NIH/NIDCR Tissue Engineering at Michigan trainee grant (DE 007057), NIH R21 DE 022439, and NIH R01 AR 060892.

Disclosure Statement

Scott J. Hollister was a co-founder of Tissue Regeneration Systems (TRS) but is no longer affiliated.

References

1. Bhumiratana, S., and Vunjak-Novakovic, G. Concise review: personalized human bone grafts for reconstructing head and face. Stem Cells Transl Med **1,** 64, 2012.
2. Warnke, P.H., Wiltfang, J., Springer, I., Acil, Y., Bolte, H., Kosmahl, M., *et al.* Man as living bioreactor: fate of an exogenously prepared customized tissue-engineered mandible. Biomaterials **27,** 3163, 2006.
3. Warnke, P.H., Springer, I.N., Wiltfang, J., Acil, Y., Eufinger, H., Wehmoller, M., *et al.* Growth and transplantation of a custom vascularised bone graft in a man. Lancet **364,** 766, 2004.
4. Terheyden, H., Knak, C., Jepsen, S., Palmie, S., and Rueger, D.R. Mandibular reconstruction with a prefabricated vascularized bone graft using recombinant human osteogenic protein-1: an experimental study in miniature pigs. Part I: Prefabrication. Int J Oral Maxillofac Surg **30,** 373, 2001.
5. Mesimaki, K., Lindroos, B., Tornwall, J., Mauno, J., Lindqvist, C., Kontio, R., *et al.* Novel maxillary reconstruction with ectopic bone formation by GMP adipose stem cells. Int J Oral Maxillofac Surg **38,** 201, 2009.
6. Alam, M.I., Asahina, I., Seto, I., Oda, M., and Enomoto, S. Prefabrication of vascularized bone flap induced by recombinant human bone morphogenetic protein 2 (rhBMP-2). Int J Oral Maxillofac Surg **32,** 508, 2003.
7. Becker, S.T., Bolte, H., Krapf, O., Seitz, H., Douglas, T., Sivananthan, S., *et al.* Endocultivation: 3D printed customized porous scaffolds for heterotopic bone induction. Oral Oncol **45,** e181, 2009.
8. Terheyden, H., Jepsen, S., and Rueger, D.R. Mandibular reconstruction in miniature pigs with prefabricated vascularized bone grafts using recombinant human osteogenic protein-1: a preliminary study. Int J Oral Maxillofac Surg **28,** 461, 1999.
9. Terheyden, H., Menzel, C., Wang, H., Springer, I.N., Rueger, D.R., and Acil, Y. Prefabrication of vascularized bone grafts using recombinant human osteogenic protein-1—part 3: dosage of rhOP-1, the use of external and internal scaffolds. Int J Oral Maxillofac Surg **33,** 164, 2004.
10. Warnke, P.H., Springer, I.N., Acil, Y., Julga, G., Wiltfang, J., Ludwig, K., *et al.* The mechanical integrity of *in vivo* engineered heterotopic bone. Biomaterials **27,** 1081, 2006.
11. Heliotis, M., Lavery, K.M., Ripamonti, U., Tsiridis, E., and di Silvio, L. Transformation of a prefabricated hydroxyapatite/osteogenic protein-1 implant into a vascularised pedicled bone flap in the human chest. Int J Oral Maxillofac Surg **35,** 265, 2006.
12. Hollister, S.J., and Murphy, W.L. Scaffold translation: barriers between concept and clinic. Tissue Eng Part B Rev **17,** 459, 2011.
13. Williams, J.M., Adewunmi, A., Schek, R.M., Flanagan, C.L., Krebsbach, P.H., Feinberg, S.E., *et al.* Bone tissue engineering using polycaprolactone scaffolds fabricated via selective laser sintering. Biomaterials **26,** 4817, 2005.
14. Wong, D.Y., Hollister, S.J., Krebsbach, P.H., and Nosrat, C. Poly(epsilon-caprolactone) and poly (L-lactic-co-glycolic acid) degradable polymer sponges attenuate astrocyte response and lesion growth in acute traumatic brain injury. Tissue Eng **13,** 2515, 2007.
15. Fitzsimmons, J. 510(k) Premarket Notification, Cover, Burr Hole, TRS Cranial Bone Void Filler. 2014; Available at: www.accessdata.fda.gov/scripts/cdrh/cfdocs/cfpmn/pmn.cfm?ID=K123633, 2014.
16. Yeo, A. 510(k) Premarket Notification, Methyl Methacrylate For Cranioplasty, Osteopore Pcl Scaffold. 2014; Available at: www.accessdata.fda.gov/scripts/cdrh/cfdocs/cfpmn/pmn.cfm?ID=K051093, 2014.
17. Partee, B., Hollister, S.J., and Das, S. Selective laser sintering process optimization for layered manufacturing of CAPA® 6501 polycaprolactone bone tissue engineering scaffolds. J Manuf Sci Eng **128,** 531, 2005.
18. Smith, M.H., Flanagan, C.L., Kemppainen, J.M., Sack, J.A., Chung, H., Das, S.S., *et al.* Computed tomography-based tissue-engineered scaffolds in craniomaxillofacial surgery. Int J Med Robot **3,** 207, 2007.
19. Schantz, J.T., Lim, T.C., Ning, C., Teoh, S.H., Tan, K.C., Wang, S.C., *et al.* Cranioplasty after trephination using a novel biodegradable burr hole cover: technical case report. Neurosurgery **58,** ONS-E176, 2006.
20. Hutmacher, D.W., Schantz, T., Zein, I., Ng, K.W., Teoh, S.H., and Tan, K.C. Mechanical properties and cell cultural response of polycaprolactone scaffolds designed and fabricated via fused deposition modeling. J Biomed Mater Res **55,** 203, 2001.
21. Mitsak, A.G., Kemppainen, J.M., Harris, M.T., and Hollister, S.J. Effect of polycaprolactone scaffold permeability on bone regeneration *in vivo.* Tissue Eng Part A **17,** 1831, 2011.
22. Zhang, H., Migneco, F., Lin, C.Y., and Hollister, S.J. Chemically-conjugated bone morphogenetic protein-2 on

three-dimensional polycaprolactone scaffolds stimulates osteogenic activity in bone marrow stromal cells. Tissue Eng Part A **16,** 3441, 2010.
23. Jeon, O., Song, S.J., Kang, S.W., Putnam, A.J., and Kim, B.S. Enhancement of ectopic bone formation by bone morphogenetic protein-2 released from a heparin-conjugated poly(L-lactic-co-glycolic acid) scaffold. Biomaterials **28,** 2763, 2007.
24. Zhang, Q., He, Q.F., Zhang, T.H., Yu, X.L., Liu, Q., and Deng, F.L. Improvement in the delivery system of bone morphogenetic protein-2: a new approach to promote bone formation. Biomed Mater **7,** 045002, 2012.
25. Park, Y.J., Kim, K.H., Lee, J.Y., Ku, Y., Lee, S.J., Min, B.M., *et al.* Immobilization of bone morphogenetic protein-2 on a nanofibrous chitosan membrane for enhanced guided bone regeneration. Biotechnol Appl Biochem **43(Pt 1),** 17, 2006.
26. Kim, T.H., Oh, S.H., Na, S.Y., Chun, S.Y., and Lee, J.H. Effect of biological/physical stimulation on guided bone regeneration through asymmetrically porous membrane. J Biomed Mater Res A **100,** 1512, 2012.
27. Liu, H.W., Chen, C.H., Tsai, C.L., and Hsiue, G.H. Targeted delivery system for juxtacrine signaling growth factor based on rhBMP-2-mediated carrier-protein conjugation. Bone **39,** 825, 2006.
28. Rai, B., Teoh, S.H., Hutmacher, D.W., Cao, T., and Ho, K.H. Novel PCL-based honeycomb scaffolds as drug delivery systems for rhBMP-2. Biomaterials **26,** 3739, 2005.
29. Gharibjanian, N.A., Chua, W.C., Dhar, S., Scholz, T., Shibuya, T.Y., Evans, G.R., *et al.* Release kinetics of polymer-bound bone morphogenetic protein-2 and its effects on the osteogenic expression of MC3T3-E1 osteoprecursor cells. Plast Reconstr Surg **123,** 1169, 2009.
30. Dias, M.R., Guedes, J.M., Flanagan, C.L., Hollister, S.J., and Fernandes, P.R. Optimization of scaffold design for bone tissue engineering: a computational and experimental study. Med Eng Phys **36,** 448, 2014.
31. Zopf, D.A., Hollister, S.J., Nelson, M.E., Ohye, R.G., and Green, G.E. Bioresorbable airway splint created with a three-dimensional printer. N Engl J Med **368,** 2043, 2013.
32. van de Watering, F.C., van den Beucken, J.J., van der Woning, S.P., Briest, A., Eek, A., Qureshi, H., *et al.* Non-glycosylated BMP-2 can induce ectopic bone formation at lower concentrations compared to glycosylated BMP-2. J Control Release **159,** 69, 2012.
33. Katagiri, T., Yamaguchi, A., Komaki, M., Abe, E., Takahashi, N., Ikeda, T., *et al.* Bone morphogenetic protein-2 converts the differentiation pathway of C2C12 myoblasts into the osteoblast lineage. J Cell Biol **127(6 Pt 1),** 1755, 1994.
34. Jiao, X., Billings, P.C., O'Connell, M.P., Kaplan, F.S., Shore, E.M., and Glaser, D.L. Heparan sulfate proteoglycans (HSPGs) modulate BMP2 osteogenic bioactivity in C2C12 cells. J Biol Chem **282,** 1080, 2007.
35. Pohl, T.L., Boergermann, J.H., Schwaerzer, G.K., Knaus, P., and Cavalcanti-Adam, E.A. Surface immobilization of bone morphogenetic protein 2 via a self-assembled monolayer formation induces cell differentiation. Acta Biomater **8,** 772, 2012.
36. Zhao, Y., Zhang, J., Wang, X., Chen, B., Xiao, Z., Shi, C., *et al.* The osteogenic effect of bone morphogenetic protein-2 on the collagen scaffold conjugated with antibodies. J Control Release **141,** 30, 2010.
37. Kontogiorgos, E., Elsalanty, M.E., Zapata, U., Zakhary, I., Nagy, W.W., Dechow, P.C., *et al.* Three-dimensional evaluation of mandibular bone regenerated by bone transport distraction osteogenesis. Calcif Tissue Int **89,** 43, 2011.
38. Cahill, K.S., Chi, J.H., Day, A., and Claus, E.B. Prevalence, complications, and hospital charges associated with use of bone-morphogenetic proteins in spinal fusion procedures. JAMA **302,** 58, 2009.
39. Santo, V.E., Gomes, M.E., Mano, J.F., and Reis, R.L. Controlled release strategies for bone, cartilage, and osteochondral engineering—Part I: recapitulation of native tissue healing and variables for the design of delivery systems. Tissue Eng Part B Rev **19,** 308, 2013.
40. Han, J., Cao, R.W., Chen, B., Ye, L., Zhang, A.Y., Zhang, J., *et al.* Electrospinning and biocompatibility evaluation of biodegradable polyurethanes based on L-lysine diisocyanate and L-lysine chain extender. J Biomed Mater Res A **96,** 705, 2011.
41. Kumagai, T., Anada, T., Honda, Y., Takami, M., Kamijyo, R., Shimauchi, H., *et al.* Osteoblastic cell differentiation on BMP-2 pre-adsorbed octacalcium phosphate and hydroxyapatite. Key Eng Mater **361,** 1025, 2007.
42. Bae, S.E., Choi, J., Joung, Y.K., Park, K., and Han, D.K. Controlled release of bone morphogenetic protein (BMP)-2 from nanocomplex incorporated on hydroxyapatite-formed titanium surface. J Control Release **160,** 676, 2012.
43. Hosseinkhani, H., Hosseinkhani, M., Khademhosseini, A., and Kobayashi, H. Bone regeneration through controlled release of bone morphogenetic protein-2 from 3-D tissue engineered nano-scaffold. J Control Release **117,** 380, 2007.
44. Kirby, G.T.S., White, L.J., Rahman, C.V., Cox, H.C., Qutachi, O., Felicity, R.A.J.R., *et al.* PLGA-based microparticles for the sustained release of BMP-2. Polymers **3,** 571, 2011.
45. Apatite-Polymer Composite Particles for Controlled Delivery of BMP-2: *In Vitro* Release and Cellular Response. Proceedings of the Singapore-MIT Alliance Symposium, Singapore, 2005.
46. Autefage, H., Briand-Mesange, F., Cazalbou, S., Drouet, C., Fourmy, D., Goncalves, S., *et al.* Adsorption and release of BMP-2 on nanocrystalline apatite-coated and uncoated hydroxyapatite/beta-tricalcium phosphate porous ceramics. J Biomed Mater Res B Appl Biomater **91,** 706, 2009.

Address correspondence to:
Scott J. Hollister, PhD
Department of Biomedical Engineering
University of Michigan
1101 Beal Avenue
2214 Lurie Biomedical Engineering
Ann Arbor, MI 48109-2110

E-mail: scottho@umich.edu

Received: June 27, 2014
Accepted: October 14, 2014
Online Publication Date: January 30, 2015

This article has been cited by:

1. Pedro Alvarez-Urena, Banghe Zhu, Gabrielle Henslee, Corinne Sonnet, Eleanor Davis, Eva Sevick-Muraca, Alan Davis, Elizabeth Olmsted-Davis. 2017. Development of a Cell-Based Gene Therapy Approach to Selectively Turn Off Bone Formation. *Journal of Cellular Biochemistry* **118**:11, 3627-3634. [Crossref]
2. Marcello Rubessa, Kathryn Polkoff, Massimo Bionaz, Elisa Monaco, Derek J. Milner, Scott J. Holllister, Michael S. Goldwasser, Matthew B. Wheeler. 2017. Use of Pig as a Model for Mesenchymal Stem Cell Therapies for Bone Regeneration. *Animal Biotechnology* **28**:4, 275-287. [Crossref]
3. Sun Woo Jung, June-Ho Byun, Se Heang Oh, Tae Ho Kim, Ji-Sung Park, Gyu-Jin Rho, Jin Ho Lee. 2017. Multivalent ion-based in situ gelling polysaccharide hydrogel as an injectable bone graft. *Carbohydrate Polymers* . [Crossref]
4. Almoatazbellah Youssef, Scott J Hollister, Paul D Dalton. 2017. Additive manufacturing of polymer melts for implantable medical devices and scaffolds. *Biofabrication* **9**:1, 012002. [Crossref]
5. Scott J. Hollister, Colleen L. Flanagan, Robert J. Morrison, Janki J. Patel, Matthew B. Wheeler, Sean P. Edwards, Glenn E. Green. 2016. Integrating Image-Based Design and 3D Biomaterial Printing To Create Patient Specific Devices within a Design Control Framework for Clinical Translation. *ACS Biomaterials Science & Engineering* **2**:10, 1827-1836. [Crossref]
6. Ru-Lin Huang, Eiji Kobayashi, Kai Liu, Qingfeng Li. 2016. Bone Graft Prefabrication Following the In Vivo Bioreactor Principle. *EBioMedicine* **12**, 43-54. [Crossref]
7. D.W. Weisgerber, K. Erning, C.L. Flanagan, S.J. Hollister, B.A.C. Harley. 2016. Evaluation of multi-scale mineralized collagen–polycaprolactone composites for bone tissue engineering. *Journal of the Mechanical Behavior of Biomedical Materials* **61**, 318-327. [Crossref]
8. Ho Yong Kim, Jin Ho Lee, Jeong-Won Yun, Jin-Ho Park, Bong-Wook Park, Gyu-Jin Rho, Si-Jung Jang, Ji-Sung Park, Hee-Chun Lee, Young Min Yoon, Tae Sung Hwang, Dong Hoon Lee, June-Ho Byun, Se Heang Oh. 2016. Development of Porous Beads to Provide Regulated BMP-2 Stimulation for Varying Durations: In Vitro and In Vivo Studies for Bone Regeneration. *Biomacromolecules* **17**:5, 1633-1642. [Crossref]
9. Sophia P. Pilipchuk, Alberto Monje, Yizu Jiao, Jie Hao, Laura Kruger, Colleen L. Flanagan, Scott J. Hollister, William V. Giannobile. 2016. Integration of 3D Printed and Micropatterned Polycaprolactone Scaffolds for Guidance of Oriented Collagenous Tissue Formation In Vivo. *Advanced Healthcare Materials* **5**:6, 676-687. [Crossref]
10. Patel Janki Jayesh, Modes Jane E., Flanagan Colleen L., Krebsbach Paul H., Edwards Sean P., Hollister Scott J.. 2015. Dual Delivery of EPO and BMP2 from a Novel Modular Poly-ε-Caprolactone Construct to Increase the Bone Formation in Prefabricated Bone Flaps. *Tissue Engineering Part C: Methods* **21**:9, 889-897. [Abstract] [Full Text HTML] [Full Text PDF] [Full Text PDF with Links]